AGU PUBLICATIONS

Global Biogeochemical Cycles

RESEARCH ARTICLE
10.1002/2016GB005613

Key Points:
- Atlantic N_2 fixation rates are calculated from nitrate isotopes and WOCE-derived nitrate transports
- N_2 fixation north of 11°S is 27.1 Tg N/yr; 90% of this rate occurs south of 24°N, responding to excess P supply
- N_2 fixation in the equatorial and North Atlantic can stabilize the global ocean N-to-P ratio, but this is not needed today

Supporting Information:
- Supporting Information S1
- Figure S1
- Figure S2
- Figure S3
- Figure S4
- Table S1

Correspondence to:
D. Marconi,
dmarconi@princeton.edu

Citation:
Marconi, D., Sigman, D. M., Casciotti, K. L., Campbell, E. C., Alexandra Weigand, M., Fawcett, S. E., … Haug, G. H. (2017). Tropical dominance of N_2 fixation in the North Atlantic Ocean. *Global Biogeochemical Cycles*, *31*, 1608–1623. https://doi.org/10.1002/2016GB005613

Received 23 DEC 2016
Accepted 6 AUG 2017
Accepted article online 15 SEP 2017
Published online 30 OCT 2017

Tropical Dominance of N_2 Fixation in the North Atlantic Ocean

Dario Marconi[1], Daniel M. Sigman[1], Karen L. Casciotti[2], Ethan C. Campbell[3], M. Alexandra Weigand[1], Sarah E. Fawcett[4], Angela N. Knapp[5], Patrick A. Rafter[6], Bess B. Ward[1], and Gerald H. Haug[7]

[1]Department of Geosciences, Princeton University, Princeton, NJ, USA, [2]Department of Environmental Earth System Science, Stanford University, Stanford, CA, USA, [3]School of Oceanography, University of Washington, Seattle, WA, USA, [4]Department of Oceanography, University of Cape Town, Rondebosch, South Africa, [5]Earth, Ocean, and Atmospheric Science Department, Florida State University, Tallahassee, FL, USA, [6]Department of Earth System, University of California, Irvine, CA, USA, [7]Max Planck Institute for Chemistry, Mainz, Germany

Abstract To investigate the controls on N_2 fixation and the role of the Atlantic in the global ocean's fixed nitrogen (N) budget, Atlantic N_2 fixation is calculated by combining meridional nitrate fluxes across World Ocean Circulation Experiment sections with observed nitrate $^{15}N/^{14}N$ differences between northward and southward transported nitrate. N_2 fixation inputs of 27.1 ± 4.3 Tg N/yr and 3.0 ± 0.5 Tg N/yr are estimated north of 11°S and 24°N, respectively. That is, ~90% of the N_2 fixation in the Atlantic north of 11°S occurs south of 24°N in a region with upwelling that imports phosphorus (P) in excess of N relative to phytoplankton requirements. This suggests that, under the modern iron-rich conditions of the equatorial and North Atlantic, N_2 fixation occurs predominantly in response to P-bearing, N-poor conditions. We estimate a N_2 fixation rate of 30.5 ± 4.9 Tg N/yr north of 30°S, implying only 3 Tg N/yr between 30° and 11°S, despite evidence of P-bearing, N-poor surface waters in this region as well; this is consistent with iron limitation of N_2 fixation in the South Atlantic. Since the ocean flows through the Atlantic surface in <2,500 years, similar to the residence time of oceanic fixed N, Atlantic N_2 fixation can stabilize the N-to-P ratio of the global ocean. However, the calculated rate of Atlantic N_2 fixation is a small fraction of global ocean estimates for either N_2 fixation or fixed N loss. This suggests that, in the modern ocean, an approximate balance between N loss and N_2 fixation is achieved within the combined Indian and Pacific basins.

1. Introduction

The potential for temporal changes in the size of the oceanic reservoir of biologically available (or "fixed") N has been debated for decades, attracting interest in part because such changes could significantly affect the biological fertility of the ocean and its role in the global carbon cycle and atmospheric CO_2 change. N_2 fixation by marine diazotrophs is the dominant fixed N input to the ocean (Gruber, 2004), such that it exerts an important potential control on the variability of the oceanic fixed N reservoir. Previous work has provided conflicting views of oceanic N_2 fixation, proposing variously that N_2 fixation is controlled by physical conditions (Carpenter & Price, 1976), iron (Falkowski, 1997; Moore et al., 2009), or "excess" P (P in excess of N relative to the typical demands of plankton, quantifiable as P*, defined as $[PO_4^{3-}]$-$[NO_3^-]/16$) (Deutsch et al., 2007; Knapp et al., 2012; Monteiro, Dutkiewicz, & Follows, 2011; Sanudo-Wilhemly et al., 2004; Straub et al., 2013). The question of what controls N_2 fixation has received additional interest due to the suggestion that the global ocean rate of N_2 fixation is far lower than that of denitrification, the main sink for oceanic fixed N (Brandes & Devol, 2002; Codispoti, 2007; Codispoti et al., 2001), which implies that the global ocean's N budget is out of balance.

The spatial distribution of N_2 fixation in the modern ocean provides insight into the parameters that control it, which has motivated the effort to identify regions of highest N_2 fixation (Capone et al., 1998; Carpenter & McCarthy, 1975; Carpenter & Price, 1977; Carpenter & Romans, 1991; Dugdale et al., 1964; Montoya et al., 2002). Developing robust estimates of the regional rate and distribution of N_2 fixation from "direct" shipboard incubations is complicated by the inherent spatial and temporal variability of this biological process as well as by the challenge of simulating oceanic conditions in incubations. For these reasons, biogeochemical properties of ocean water have become important as integrative measures of N_2 fixation as well as of other N fluxes. Deviations from the canonical "Redfield" nitrate concentration-to-phosphate concentration

($[NO_3^-]$-to-$[PO_4^{3-}]$) relationship driven by assimilation and remineralization have been used to study the rates and magnitudes of both N_2 fixation and denitrification. Regional rates of N_2 fixation have been derived by combining spatial variations in the $[NO_3^-]$-to-$[PO_4^{3-}]$ relationship (often expressed using N*, defined as $[NO_3^-] - 16 \times [PO_4^{3-}] + 2.9$ μmol/kg; Gruber & Sarmiento, 1997) with measures of the rate of ocean circulation (Gruber & Sarmiento, 1997; Hansell et al., 2004, 2007; Michaels et al., 1996). While this application of nutrient concentration data is powerful, it has limitations. First, deviations from the Redfield $[NO_3^-]$-to-$[PO_4^{3-}]$ relationship may not always be due to N inputs or losses, arising instead from variations in the stoichiometry of nutrient uptake and remineralization (Martiny et al., 2013; Mills & Arrigo, 2010; Weber & Deutsch, 2010, 2012). Second, $[NO_3^-]$-to-$[PO_4^{3-}]$ ratio signals of N_2 fixation and N loss can erase each other if they occur in the same regions or if their host waters are mixed in a way that cannot be reconstructed.

The N isotopes of nitrate provide a complementary geochemical approach for reconstructing regional rates of N_2 fixation (e.g., Knapp et al., 2008). Newly fixed N has a $\delta^{15}N$ that is similar to that of atmospheric N_2 (~ −2 to 0‰, Carpenter et al., 1997; Delwiche et al., 1979; Hoering & Ford, 1960; Minagawa & Wada, 1986; $\delta^{15}N$ (‰) = $\{[(^{15}N/^{14}N)_{sample}/(^{15}N/^{14}N)_{reference}] - 1\} \times 1{,}000$, where the reference is atmospheric N_2). In contrast, deep ocean NO_3^- has a mean $\delta^{15}N$ of ~5‰, due to isotopic fractionation during water column denitrification (Brandes & Devol, 2002). Regionally, the addition of newly fixed N, followed by its export as organic N into the subsurface, remineralization to ammonium, and nitrification to nitrate, should lower the $\delta^{15}N$ of nitrate in the ocean interior. Indeed, there is evidence for ingrowth of low-$\delta^{15}N$ nitrate into the thermocline waters of both the North Atlantic (Bourbonnais et al., 2009; Karl et al., 2002; Knapp et al., 2008, 2005; Marconi et al., 2015) and the North Pacific (e.g., Casciotti et al., 2008; Liu et al., 1996; Sigman et al., 2009; Wong et al., 2002), which is qualitatively consistent with the large-scale patterns in N* that suggest either local or regional inputs from N_2 fixation.

Estimating the rate of N_2 fixation from a geochemical tracer, whether N* or nitrate $\delta^{15}N$, requires information on ocean circulation and exchange between water parcels. Gruber and Sarmiento (1997) used tritium/helium ages to estimate North Atlantic N_2 fixation from N* gradients along isopycnals. As an alternative approach, numerical models of ocean circulation have been used to convert N* and/or nitrate $\delta^{15}N$ measurements into estimates of the rate and spatial distribution of N_2 fixation (Coles & Hood, 2007; Deutsch et al., 2007, 2004; DeVries et al., 2013; Eugster & Gruber, 2012; Knapp et al., 2008).

Here we use recently produced nitrate $\delta^{15}N$ depth sections to reconstruct the north/south distribution of N_2 fixation for much of the Atlantic Ocean. Our constraint on ocean circulation comes from calculations of transport across zonal hydrographic sections of the World Ocean Circulation Experiment (WOCE) (Ganachaud, 2003). The premise is that without the addition of newly fixed N to the Atlantic, the nitrate $\delta^{15}N$ of newly formed North Atlantic Deep Water (NADW) would be high (~5.7‰) due to the high nitrate $\delta^{15}N$ of northward flowing Subantarctic Mode Water (SAMW) and Antarctic Intermediate Water (AAIW) that represent the dominant feed water for NADW (Marconi et al., 2015). However, the $\delta^{15}N$ of nitrate in NADW and its immediate North Atlantic source region are not elevated relative to the global mean, indicating that the high nitrate $\delta^{15}N$ of SAMW and AAIW are overprinted by the addition of low-$\delta^{15}N$ nitrate. Thus, the lower $\delta^{15}N$ of nitrate being transported southward (mainly as NADW) relative to that being transported northward across each WOCE section is interpreted to result from N_2 fixation occurring north of the section (Figure 1).

2. Methods

2.1. Nitrate Isotope Data Sets

The $\delta^{15}N$ of northward and southward transported nitrate at five zonal WOCE sections (A10, A8, A6, A5, and A2) is estimated using nitrate $\delta^{15}N$ data measured along four different transects of the Atlantic Ocean (Figure 2): CLIVAR A16N (this study; Marconi, 2017), U.S. GEOTRACES (GA03) (Marconi et al., 2015), CoFeMUG (http://www.bco-dmo.org/dataset/630246/data), and South Atlantic MOC Basin-wide Array (SAMBA) (Ansorge et al., 2014; Campbell, 2016). For all of these transects, water samples were analyzed for nitrate $\delta^{15}N$ using the "denitrifier method" (Casciotti et al., 2002; McIlvin & Casciotti, 2011; Sigman et al., 2001; Weigand et al., 2016). The nitrate $\delta^{15}N$ data along the A16N transect used for the calculations described in this section will be provided to the Biological and Chemical Oceanography Data Management Office upon publication.

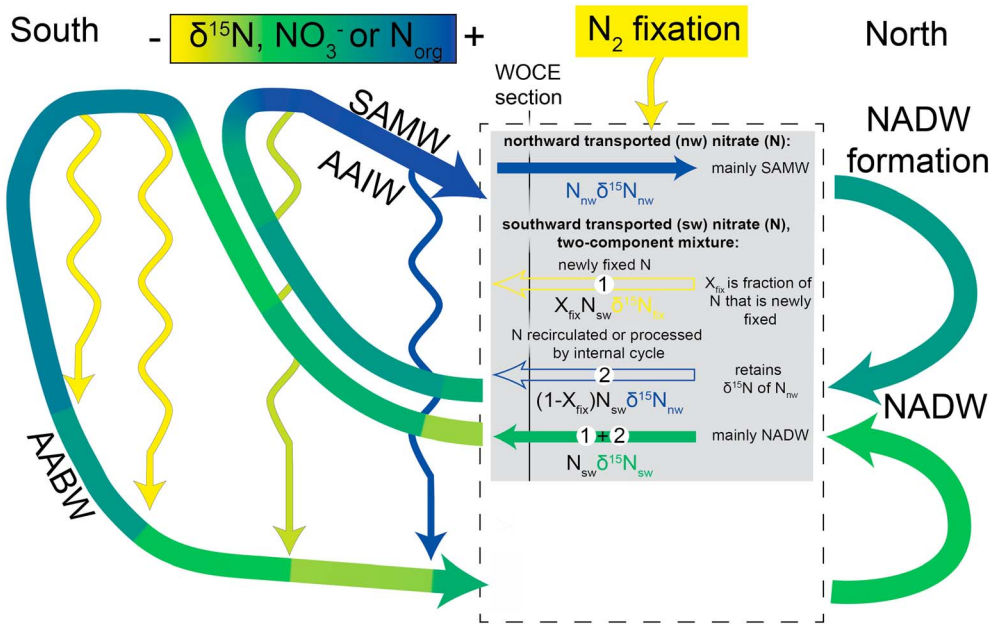

Figure 1. The $\delta^{15}N$ of nitrate and sinking organic N associated with the meridional components of ocean circulation in the Atlantic basin. The circulation approximately balances water masses flowing northward at intermediate and abyssal depths (AAIW + SAMW and Antarctic Bottom Water (AABW), respectively) and NADW flowing southward at deep levels. The colors highlight the $\delta^{15}N$ changes that nitrate undergoes along the circulation (blue, high $\delta^{15}N$; yellow, low $\delta^{15}N$). Wavy arrows indicate the rain of organic matter and its remineralization. Partial nitrate consumption by Southern Ocean phytoplankton elevates the $\delta^{15}N$ of the nitrate entering the South Atlantic in AAIW + SAMW and weakly lowers the $\delta^{15}N$ of AABW; the former dominates, yielding a high $\delta^{15}N$ for nitrate flowing northward. N_2 fixation in the Atlantic prevents NADW nitrate from inheriting this high $\delta^{15}N$ (Marconi et al., 2015). The fraction of newly fixed nitrate in southward flowing waters (NADW) is calculated using a nitrate isotopic mass balance (box with dashed outline; see text).

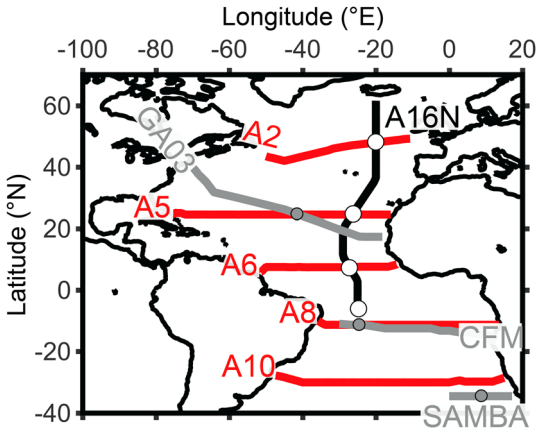

Figure 2. Field observations used in this work to calculate the $\delta^{15}N$ of northward- and southward-transported nitrate at five WOCE sections (A2 at 48°N, A5 at 24°N, A6 at 7.5°N, and A8 at 11°S; red lines). The meridional A16N transect extends from south of Iceland to 6°S in the tropical Atlantic and yields cross points with four WOCE sections (white-filled circles). Zonal sections associated with U.S. GEOTRACES (GA03) (Marconi et al., 2015), CoFeMUG (CFM) (http://www.bco-dmo.org/dataset/630246/data), and the South Atlantic MOC Basin-wide Array (SAMBA) (Campbell, 2016) provide additional cross points with three WOCE sections (A5, A8, and A10; grey-filled circles). At WOCE A5, A8, and A10, the $\delta^{15}N$ of northward and southward transported nitrate is also calculated via two additional approaches ("section" and "semisection" methods), using all stations from GA03, CoFeMUG, and SAMBA zonal transects (grey lines).

The data set along the A16N transect is the starting point for our calculations (Figure 2, black line; Figure 3). This meridional transect was sampled in 2013 and extends from south of Iceland to 6°S in the tropical Atlantic, providing cross points with four different WOCE sections (A2 at 48°N, A5 at 24°N, A6 at 7.5°N, and A8 at 11°S; Figure 2, open circles "cross-station approach"). A16N stations within 2° of latitude of each WOCE section are used in our calculations, with the exception of A8, for which the southernmost A16N stations are used. All cross points are located in the central or central eastern Atlantic, with longitudes between 20°W and 27°W.

The GA03 section used with WOCE A5 (Marconi et al., 2015) and the CoFeMUG section used with WOCE A8 represent nitrate $\delta^{15}N$ sections that are more zonal but lower in depth resolution (Figures 2, 3b, and 3c). These transects allow for calculations analogous to those using A16N but with different cross points (Figure 2, grey circles). Moreover, GA03 and CoFeMUG data are used to directly compare the cross-station approach with calculations that include the observed zonal gradients in nitrate $\delta^{15}N$ ("section approach").

Unlike for the other zonal transects, the calculations performed with SAMBA nitrate $\delta^{15}N$ data do not test the A16N-based calculations. The SAMBA transect, completed in 2015, extends from 0 to 17°E at 34.5°S, being the only data set of this work to provide nitrate $\delta^{15}N$ data near the location of WOCE section A10 (30°S) (Figure 2 and supporting information Figure S1). This boundary permits a preliminary calculation

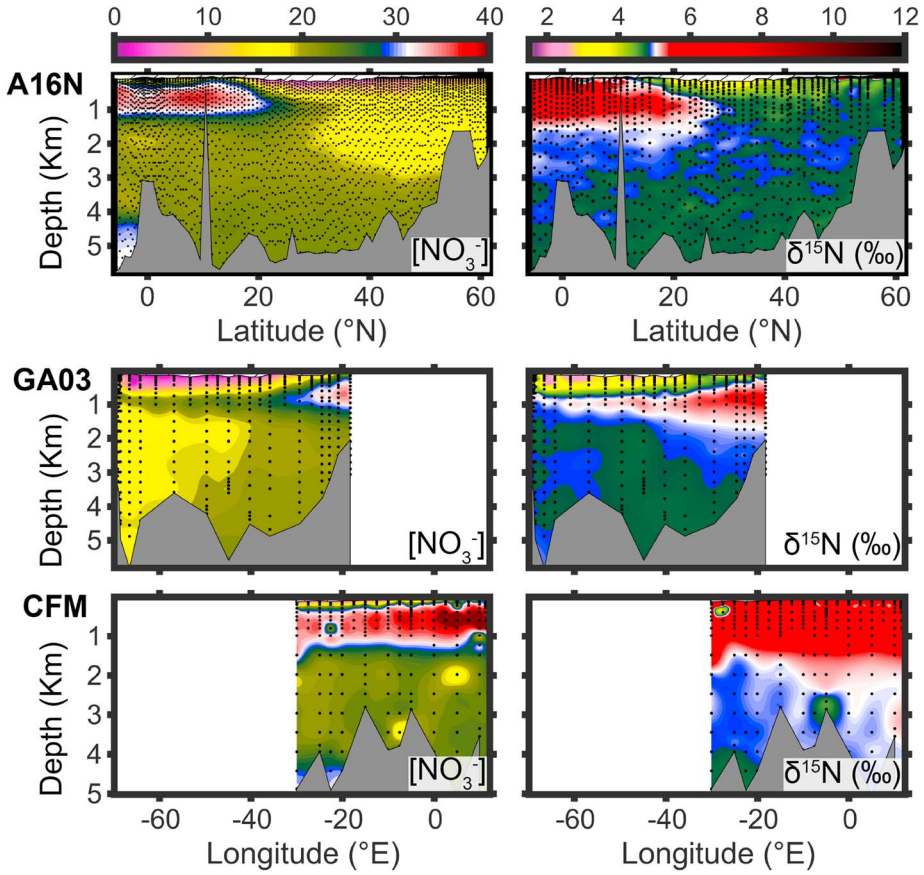

Figure 3. Depth sections of (left column) nitrate concentration and (right column) δ^{15}N from three data sets used in this work. (top row) The data from the meridional A16N transect are displayed versus latitude. (middle and bottom rows) The data from the zonal GA03 and CoFeMUG (CFM) sections are shown versus longitude.

of the N_2 fixation rate in the Atlantic as a whole and allows the N_2 fixation rates from northward of 11°S to be assessed relative to that estimate. We refer below to the SAMBA analysis as using a "semisection approach," in that data are used from across this section, but the section does not cross the basin and does not exactly overlap with WOCE A10.

2.1.1. Calculations

Our calculations use horizontal volume transports at each WOCE section, estimated for 17 or 18 neutral density intervals ("density classes") by Ganachaud and Wunsch (2000) and Ganachaud (2003) (http://www.legos.obs-mip.fr). In the A16N-based cross-station approach, volume-mean nitrate concentration and δ^{15}N for each density class are calculated from the A16N stations at the cross points. These values are combined with the transports to yield the nitrate concentration and δ^{15}N of total northward and southward flows (supporting information section S1.1). In order to calculate the N_2 fixation rate north of each section, we assume that the nitrate in the southward flow (N_{sw}, the concentration of nitrate in southward flowing water) is a mixture of (a) newly fixed nitrate with a δ^{15}N ($\delta^{15}N_{fix}$) of -1 ± 1‰ and (b) nitrate with the same δ^{15}N as that of nitrate in the northward flow ($\delta^{15}N_{nw}$) (Figure 1). The rationale for (b) is that the fraction of N_{sw} that is not newly fixed N is nitrate that had previously crossed the section from the south and was either recirculated or underwent cycles of consumption and remineralization to be converted into regenerated nitrate, in either case conserving its δ^{15}N, $\delta^{15}N_{nw}$. By defining X_{fix} as the fraction of N_{sw} that originates from newly fixed N, we can write the following mass balance equation:

$$N_{sw} \times \delta^{15}N_{sw} = X_{fix} \times N_{sw} \times \delta^{15}N_{fix} + (1 - X_{fix}) \times N_{sw} \times \delta^{15}N_{nw} \quad (1a)$$

From equation (1a), we derive X_{fix}, the fraction of N_{sw} that was fixed north of the section rather than having entered that region by circulation from the south:

Table 1
$\delta^{15}N$ of Northward- and Southward-Transported Nitrate and Calculated Rates of N_2 Fixation

WOCE section	Method	$\delta^{15}N$ (nw[a]) (‰ versus air)	$\delta^{15}N$ (sw[b]) (‰ versus air)	N_2 fix. rate[c] (Tg N/yr)
A2 (48°N)	A16N cross station (20°W)	4.82	4.81	0.4 ± 0.5
A5 (24°N)	A16N cross station (27°W)	4.94	4.84	3.0 ± 0.5
	GA03 cross station (40°W)	4.86	4.82	1.2 ± 0.2
	GA03 averaged section	5.05	4.85	5.4 ± 1.0
	GA03 resolved section	5.03	4.83	5.4 ± 1.0
A6 (7.5°N)	A16N cross station (27°W)	5.34	4.84	12.2 ± 2.6
A8 (11°S)	A16N cross station (25°W)	5.78	4.99	27.1 ± 4.3
	CoFeMUG cross station (25°W)	5.84	4.97	30.4 ± 5.1
	CoFeMUG averaged section	5.84	5.01	29.4 ± 5.0
	CoFeMUG resolved section	5.84	5.01	29.1 ± 4.9
A10 (30°S)	SAMBA semisection	5.81	5.04	30.5 ± 4.9

[a]Northward. [b]Southward. [c]Average plus/minus one standard deviation.

$$X_{fix} = \left(\delta^{15}N_{sw} - \delta^{15}N_{nw}\right)/\left(\delta^{15}N_{fix} - \delta^{15}N_{nw}\right) \quad (1b)$$

The rate of N_2 fixation (N_{fix}) north of the section is then obtained by multiplying X_{fix} by the total southward transport:

$$N_{fix} = \left(X_{fix} \times N_{sw} \times Sv_{sw}\right) \quad (1c)$$

The calculations performed combining nitrate concentration and nitrate $\delta^{15}N$ data from the A16N transect and transports from WOCE sections A8, A6, A5, and A2 are summarized in Table 1. The rate of N_2 fixation in the domain north of each WOCE section is given by the calculation for each section. The rate of N_2 fixation for a region between adjacent WOCE sections is calculated by subtracting the rate north of the northern boundary from the rate north of the southern boundary of the region.

For the rate of N_2 fixation north of each WOCE section calculated using the cross-station approach, averages and uncertainty intervals include three sources of uncertainty: (1) the $\delta^{15}N$ of newly fixed N, (2) the calculated transports, and (3) the use of nitrate concentration data from cross stations instead of full sections (Table 1 and supporting information Table S1 and Figure S2). First, to address the uncertainty in the $\delta^{15}N$ of newly fixed N from N_2 fixation, the rate is also calculated assigning values of 0‰ and −2‰ to the $\delta^{15}N$ of newly fixed N ($\delta^{15}N_{fix}$) in order to account for the range of values suggested by field and culture data on open ocean diazotrophs (Carpenter et al., 1997; Delwiche et al., 1979; Hoering & Ford, 1960). The uncertainty in $\delta^{15}N_{fix}$ introduces an uncertainty in the N_2 fixation rate estimates of roughly ±15% of the calculated rate. While nontrivial at the quantitative level, it influences neither the spatial pattern in N_2 fixation estimates nor the key findings from the comparison of our calculated rates to estimates of the global ocean rate of N_2 fixation. Second, as one approach to address uncertainty in the calculated transports, the last step of our calculations ($X_{fix} \times N_{sw} \times Sv_{sw}$) is repeated replacing the total transport of the southward flow (Sv_{sw}) with the total transport of the northward flow (Sv_{nw}). Third, as a first investigation of the error associated with using cross stations as opposed to full parallel sections for the biogeochemical data, the rates of N_2 fixation obtained are recalculated using WOCE nitrate concentration data from the full WOCE section instead of A16N measurements at the cross stations.

While the use of a single meridional section of nitrate isotopes (i.e., A16N) is beneficial from the perspective of consistency between the analyses at the different WOCE sections, a corresponding weakness is its reliance on data from a single longitude. Within the same density level, the nitrate $\delta^{15}N$ of A16N samples at those stations is taken as representative of the nitrate $\delta^{15}N$ across each WOCE zonal section. This assumption is reasonable given the general observation that both the concentration and $\delta^{15}N$ of nitrate change most strongly as a function of latitude and density interval rather than longitude in the Atlantic (Figure 3). Nevertheless, to

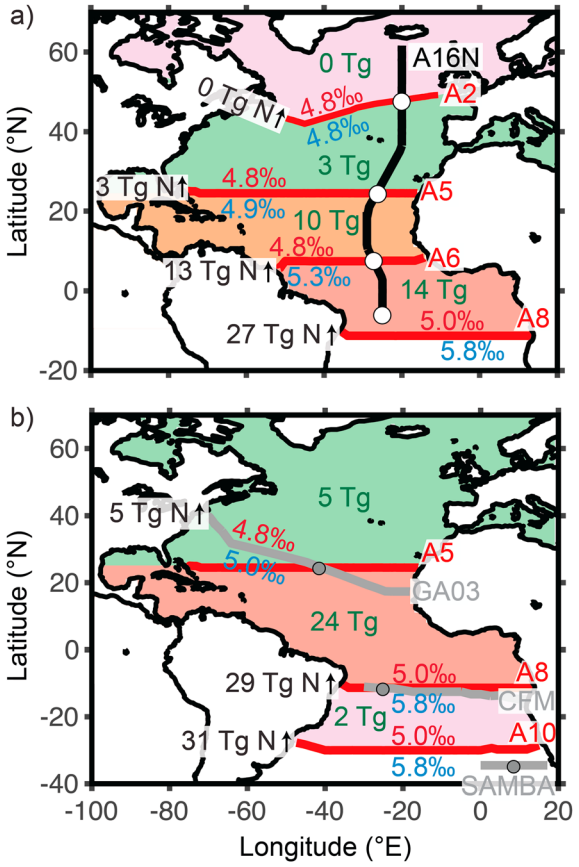

Figure 4. The $\delta^{15}N$ of northward- and southward-transported nitrate calculated at the WOCE sections (blue and red numbers, respectively) and distribution of reconstructed N_2 fixation rates for the Atlantic. Black numbers (with arrows) indicate the total N_2 fixation rate calculated north of WOCE sections, while green numbers indicate the N_2 fixation rate between two adjacent WOCE sections (in units of 10^{12} g (teragram, Tg) N per year). (a) The $\delta^{15}N$ of transported nitrate and the N_2 fixation rates calculated using the A16N data with the cross-station method. (b) The $\delta^{15}N$ of transported nitrate and N_2 fixation rates calculated with GA03, CoFeMUG (CFM), and SAMBA data using the section and the semisection methods.

test the robustness of the calculations, the fluxes obtained using A16N data are recalculated for WOCE A5 at 24°N and A8 at 11°S using nitrate $\delta^{15}N$ data from the GA03 section (Marconi et al., 2015) for A5 and the CoFeMUG section (http://www.bco-dmo.org/dataset/630246/data) for A8. Two sets of alternative calculations are performed (Table 1). The first alternative is identical to the cross-point approach taken above, except that the cross points of the GA03 and CoFeMUG transects with WOCE sections A5 and A8 are at different locations than with A16N (Table 1). The cross point of GA03 with A5 has the same latitude (24°N) but a more westerly longitude (~40°W) than its analogue for A16N (~27°W). The cross point of CoFeMUG with WOCE A8 has the same longitude as its analogue for A16N (25°W); however, its latitude is farther south (11°S), at the same latitude of A8, unlike the southernmost data used from A16N (6°S) (Figure 2).

The second set of alternative calculations includes two additional tests to evaluate the impact of zonal gradients in nitrate concentration and $\delta^{15}N$ that are not addressed by the cross point calculations. In these exercises, the nitrate concentration and $\delta^{15}N$ of the density classes of A5 and A8 are recalculated using all the stations of the GA03 and the CoFeMUG zonal transects ("averaged section" and "resolved section" approaches in Table 1). In the case of the averaged section approach, the calculations are identical to those of the cross-station approach, except that nearly all of the nitrate concentration and $\delta^{15}N$ data from the GA03 and CoFeMUG transects are used (all black points in the GA03 and CoFeMUG panels of Figure 3 are included in the calculations). In addition to taking advantage of this larger data set of observations, the resolved section approach correlates the zonal variations in estimated transport with the zonal variations in nitrate concentration and $\delta^{15}N$. In this case, the available zonal resolution in nitrate concentration and $\delta^{15}N$ is paired with the same zonal resolution in the calculated transport of density classes from the relevant WOCE section. With this pairing, the nitrate concentration and $\delta^{15}N$ assigned to each density class are weighted according to the longitudes in the WOCE section with more rapid transport (supporting information section S1.1). In both section approaches, samples used to calculate the volume-mean nitrate concentration and $\delta^{15}N$ in each density class span approximately the same range in longitude as the transport data from WOCE sections A5 and A8 (from 18°W to 70°W for GA03 and from 12°E to 30°W for CoFeMUG).

3. Results

The results of N transports and N_2 fixation rates calculated using the A16N cross stations are shown in Figure 4a. The results of section approaches with GA03 and CoFeMUG as well as the semisection approach with SAMBA are shown in Figure 4b. The entire suite of calculations performed in this study, including the analyses with the GA03 and CoFeMUG data using both the cross station and section approaches, is listed in Table 1.

3.1. $\delta^{15}N$ of Nitrate Transported Across WOCE Sections

From the analysis of cross points of A16N with WOCE sections A2, A5, A6, and A8, the $\delta^{15}N$ of northward-transported nitrate declines northward from 5.8‰ at 11°S (A8) to 4.8‰ at 48°N (A2) (blue numbers in Figure 4a). Most of the decline has occurred by 24°N (4.9‰ at A5). The $\delta^{15}N$ of southward flowing nitrate changes far less, with a value of 4.8‰ for all but the southernmost WOCE section A8, at which it is 5.0‰ (red numbers in Figure 4a). Accordingly, the nitrate $\delta^{15}N$ difference between southward and northward flow is greatest for the two southernmost sections, where northward transported nitrate $\delta^{15}N$ is higher than

southward transported nitrate $\delta^{15}N$ (A16N cross-station approach in Table 1). The addition of SAMBA and WOCE A10 at 30°S yields the same nitrate $\delta^{15}N$ for northward and southward transport and therefore the same $\delta^{15}N$ difference between northward and southward flow as observed at 11°S (respectively, 5.8‰, 5.0‰, and 0.8‰; Table 1 and Figure 4b).

The calculations using WOCE instead of A16N nitrate concentration data yield no change in the $\delta^{15}N$ of northward and southward flows for A6 and A8 (supporting information Table S1). The results for A2 and A5 are similar but not identical, with slightly higher $\delta^{15}N$ for the northward flow compared to the case where A16N nitrate concentration is used for the calculations (4.9‰ instead of 4.8‰ at A2 and 5.0‰ instead of 4.9‰ at A5). Using the GA03 data at A5 (24°N) or the CoFeMUG data at A8 (11°S) for the cross-point analysis does not change the $\delta^{15}N$ of the northward or southward flows at either section (Table 1 and Figure 4). Thus, the exact longitude of the cross station does not appear to be a major source of uncertainty. If the full section nitrate $\delta^{15}N$ data from the GA03 zonal transect are used at A5 (24°N), the nitrate $\delta^{15}N$ of the northward flow is 0.1‰ higher than in the cross-point analysis with either A16N or GA03 (5.0‰; Table 1 and Figure 4b). We suspect that this difference is due to the extent of the meridional domain of the GA03 transect (from 17°N in the east to 39°N in the west; Figure 2). This wide latitude range impacts our calculation because the $\delta^{15}N$ of nitrate in northward flowing SAMW- and AAIW-derived water rapidly declines toward the north (Figure 3). The inclusion of GA03 stations south of 24°N (to the east of the crossing with A5) drives the ~0.1‰ difference in $\delta^{15}N$ of the northward flow. Because the water south of 24°N is relatively nitrate-rich, this effect may be only partially compensated for by the low-$\delta^{15}N$ nitrate of GA03 stations from relatively nitrate-poor waters north of 24°N (to the west of the crossing with A5). In support of this interpretation of the difference between the cross station and section approaches for WOCE A5, the averaged and resolved section analysis with the CoFeMUG transect, which is more zonal than GA03 (Figure 2), yields results for the $\delta^{15}N$ of nitrate in northward and southward flowing water of WOCE A8 that are identical to those for both A8 cross-station analyses (Table 1).

3.2. N_2 Fixation Rates

The rate of N_2 fixation for the equatorial and North Atlantic is represented by the N_2 fixation rate north of A8 (11°S), which we calculate from the A16N data with the cross-station approach to be 27 Tg N/yr (Table 1; black number and arrow left of WOCE section A8 in Figure 4a). The results of the A16N cross-point analyses indicate that most of the N_2 fixation north of 11°S (~90%) is focused in the equatorial Atlantic and the tropical North Atlantic (14 Tg N/yr between A8 at 11°S and A6 at 7.5°N and 10 Tg N/yr between A6 at 7.5°N and A5 at 24°N), with a small fraction of the total (~10%) occurring in the subtropical North Atlantic (3 Tg N/yr between A5 at 24°N and A2 at 48°N). Our calculations also indicate that no N_2 fixation occurs north of 48°N (A16N cross-station approach estimate given in Table 1 and Figure 4a).

The distribution of N_2 fixation calculated using the cross-point approach with GA03 and CoFeMUG yields very similar results (Table 1). The N_2 fixation rate north of A8 at 11°S is calculated to be 30 Tg N/yr (Table 1), only 3 Tg N/yr higher than that calculated from the A16N cross point. The calculated N_2 fixation rate north of 24°N is 2 Tg N/yr lower than that calculated with the A16N cross point (1 Tg N/yr as opposed to 3 Tg N/yr). Overall, using the cross-point approach, the GA03 and CoFeMUG data suggest slightly stronger focusing of N_2 fixation in the equatorial and tropical North Atlantic than do the A16N data.

The results of the averaged and resolved section approaches are remarkably consistent with the cross point-based calculations, with the section approach suggesting a slightly higher rate of N_2 fixation north of 24°N than do the cross-point approaches (Table 1). Given the significant latitude range of GA03, which contrasts with the lack of latitude range in WOCE A5, we suspect that the cross-point results are more accurate. In general, all of the data sets and approaches studied here yield quite similar estimates of N_2 fixation rate.

The N_2 fixation rate calculated for the whole Atlantic basin based on WOCE A10 and SAMBA is 30.5 Tg N/yr (Figure 4b), only ~1 Tg N/yr higher than that calculated north of 11°S (CoFeMUG averaged section). Stoichiometric approaches have also suggested that N_2 fixation rates in the South Atlantic are modest or minor (Deutsch et al., 2007; Moore et al., 2009; Sohm et al., 2011). The specific eastern South Atlantic region sampled by SAMBA is particularly important for the communication of the Atlantic with the rest of the global ocean (Biastoch et al., 2008; Dencausse et al., 2010; Gordon, 1986). Nevertheless, it will be important to test this interpretation with additional nitrate isotope data near WOCE A10.

4. Interpretation and Discussion

4.1. Uncertainties

One obvious source of uncertainty in using the transport data across the WOCE zonal sections to calculate N_2 fixation rates for the Atlantic is that the estimated transports have substantial errors and incompletely characterized temporal variability. In previous work, net transports of nitrate or N* were used to estimate N_2 fixation rates for the Atlantic based on differencing the southward and the northward gross transports. The uncertainties in the gross transports rendered their small difference extremely uncertain in a proportional sense, and therefore, the N_2 fixation estimates based on this difference were too uncertain to be informative (Ganachaud & Wunsch, 2002). In our approach, the fraction of newly fixed nitrate is first calculated from the difference in $\delta^{15}N$ (not in rate) between the nitrate transport northward and southward (equation (1b); see also Figure 1). The fraction of newly fixed nitrate in southward flowing waters is then multiplied by the gross southward flux to obtain the rate of N_2 fixation north of each section (equation (1c)). Our calculations, therefore, have uncertainties related to the gross meridional transports across zonal sections, not the small and proportionally uncertain difference between southward and northward transports.

Water column denitrification markedly raises nitrate $\delta^{15}N$ (Cline & Kaplan, 1975), such that estimating N_2 fixation with the nitrate isotopes in regions with significant rates of water column denitrification requires accounting for its isotopic impact (e.g., Sigman et al., 2005). In the Atlantic, this aspect represents a minor source of uncertainty due to the lack of significant rates of water column denitrification. As a first line of evidence for this lack, the oxygen minimum zones (OMZs) of the Atlantic exhibit minima in oxygen concentration varying between ~20 μmol/kg (measured at 12°S) and ~40 μmol/kg (measured at 9°N) (Karstensen et al., 2008), far from suboxia, thus arguing against a significant role for water column denitrification. This view is supported by the observation that the Atlantic OMZs do not exhibit local/regional minima in N* that would be suggestive of a significant impact by water column denitrification (Olsen et al., 2016); instead, the lowest N* in Atlantic is associated with northward flowing AAIW, most likely a signal from the Indo-Pacific (Marconi et al., 2015). The hydrographic data do not rule out the possibility that water column denitrification is occurring in isolated environments within the Atlantic, such as on the west African shelf, but they do argue against significant basin-scale rates.

Benthic denitrification is thought to be significant in the Atlantic (e.g., Bianchi et al., 2012). This N loss, when it occurs outside of highly productive regions, generally occurs with very weak net isotopic fractionation (Brandes & Devol, 1997, 2002; Lehmann et al., 2004, 2005, 2007; Sebilo et al., 2003; Sigman et al., 2001). In this study, we are effectively assuming a benthic denitrification isotope effect of 0‰. This is not universally true and is most likely to be violated in high-latitude margin environments (Alkhatib et al., 2012; Granger et al., 2011). A nonzero isotope effect for benthic denitrification would cause our calculations to underestimate the N_2 fixation rate in the North Atlantic. The rationale is that a nitrate $\delta^{15}N$ increase due to benthic denitrification would partially offset the $\delta^{15}N$ lowering caused by N_2 fixation in the basin. However, any underestimation of N_2 fixation is likely to be small; we calculate an upper limit of 6 Tg N/yr for the Atlantic north of 34°S (supporting information section S1.2 and Figure S3).

Isotopic fractionation associated with the processes of the ocean's internal N cycling, such as partial nitrate consumption in surface waters or preferential remineralization of low-$\delta^{15}N$ N from sinking or suspended particulate N, cannot significantly influence the $\delta^{15}N$ of depth-integrated water column nitrate (Knapp et al., 2005; Sigman et al., 2009). For partial nitrate consumption to have an effect, nitrate would need to be imported into the euphotic zone on one side of one of the WOCE sections and partially consumed by phytoplankton, with the remaining nitrate then being advected across the section. In the temperate to tropical ocean, this does not occur to a significant degree. While this process is relevant close to the equatorial upwelling region (e.g., Rafter & Sigman, 2016), the low nitrate concentrations in the equatorial Atlantic surface ensure that there is very little transport of partially consumed nitrate across any one of the investigated sections. Even with such a sequence of events, the N_2 fixation estimate would only be impacted if a significant fraction of organic N resulting from the partial nitrate assimilation was also transported laterally across the section. Otherwise, this organic N would be remineralized back to nitrate on the side of the section in which partial nitrate consumption occurred, producing low $\delta^{15}N$ nitrate that compensates for the rise in nitrate $\delta^{15}N$ from partial nitrate consumption. Given the relatively low concentration of particulate

organic N observed in the open ocean, this compensation must be nearly complete, with net transports of dissolved organic N (DON) representing the only remaining concern.

DON dominates the nonnitrate fixed N pool in oceanic waters, and its concentration is elevated in the surface ocean relative to the interior (Hansell & Follows, 2008). Including dissolved organic matter in some ocean models has been found to significantly influence stoichiometric reconstructions of the intrabasin distribution of N_2 fixation, although not in the Atlantic (Deutsch et al., 2007). DON $\delta^{15}N$ is quite invariant on small spatial and temporal scales (Bourbonnais et al., 2009; Knapp et al., 2008, 2005) but varies between ocean basins, with the $\delta^{15}N$ of DON near Bermuda being ~1‰ lower than near Hawaii (Knapp et al., 2011). The existing data indicate that surface ocean DON $\delta^{15}N$ covaries with the $\delta^{15}N$ of shallow subsurface nitrate (Knapp et al., 2011). Thus, we would expect a slightly higher $\delta^{15}N$ for surface DON in the South Atlantic, decreasing toward the subtropical North Atlantic. If included in our calculations, DON would tend to increase the calculated N_2 fixation rate where the rates are highest. Given the modest concentration of DON ($\leq$4.5 μmol/kg) relative to subsurface nitrate ($\leq$35 μmol/kg), this effect would likely be minor or insignificant. The evidence for depth gradients in the $\delta^{15}N$ of DON is not as yet very compelling, with an apparent 0.2‰ rise in $\delta^{15}N$ from the surface mixed layer down to 250 m near Bermuda (Knapp et al., 2005). Given the current state of knowledge, we cannot foresee the role that depth gradients in DON $\delta^{15}N$ could play in N isotope budgeting; however, the low concentrations of and apparently modest isotopic gradients in DON do not suggest a strong impact.

In sum, while the approach pursued here includes various uncertainties, which can and will be addressed as additional data are collected, the overall rate and spatial distribution of N_2 fixation within the Atlantic are robust against the identified uncertainties.

4.2. Atmospheric N Deposition

We have treated N_2 fixation as the sole process that lowers the $\delta^{15}N$ of the Atlantic thermocline. However, the atmospheric deposition of anthropogenic N, which has been demonstrated to have a $\delta^{15}N$ similar to or lower than oceanic N_2 fixation (e.g., Hastings & Sigman, 2003; Knapp et al., 2010; Turekian, 2000), is an additional source of new N to the surface Atlantic. There is broad interest in the possibility that the atmospheric deposition of anthropogenic N significantly contributes to the low $\delta^{15}N$ of thermocline nitrate in the Atlantic. The size of this impact can be evaluated by comparing the available estimates for the deposition of atmospheric N to the North Atlantic with our N_2 fixation rate calculated north of 11°S (29 Tg N/yr). A multimodel evaluation for the year 2000 (Dentener et al., 2006), when averaged for the Atantic Ocean area north of 11°S, indicates an atmospheric input of total reactive N of ~9 Tg N/yr (supporting information Figure S4). This is a substantial fraction of our estimate for N_2 fixation north of 11°S (~30% of the total rate of 29 Tg N/yr). In addition, the low $\delta^{15}N$ of atmospheric N deposition (measured as $-$2.3‰ for total reactive N at Bermuda; Knapp et al., 2010) may make this N source slightly more effective than N_2 fixation in lowering the $\delta^{15}N$ of nitrate in thermocline waters. However, recent work suggests that atmospheric N inputs to the subtropical North Atlantic have been overestimated by as much as a factor of 3 by Dentener et al. (2006), due to recycling of N between the atmosphere and surface ocean (Altieri et al., 2016). If this is the case, atmospheric N input to the North Atlantic would be closer to ~3 Tg N/yr (~10% of the rate of N_2 fixation estimated north of 11°S). There are additional indications that atmospheric N deposition is relatively unimportant. For example, foraminifera-bound N isotope measurements suggest that previous interglacial periods were characterized by nitrate $\delta^{15}N$ in the tropical North Atlantic as low as or lower than core top values (Straub et al., 2013), arguing that the low $\delta^{15}N$ observed today does not require significant anthropogenic atmospheric N deposition.

The current study provides important additional constraints on this question. Specifically, the dominant region of low-$\delta^{15}N$ N input identified here (the low-latitude region; Figure 4a) does not correspond with the spatial pattern of anthropogenic/continentally sourced N (e.g., as estimated by Dentener et al., 2006; supporting information Figure S4). Models and measurements of reactive N deposition highlight three hot spots in the Atlantic: regions of high deposition adjacent to Europe and North America north of 30°N and one weaker maximum around the equator near the coast of Africa (Chien et al., 2016; Dentener et al., 2006). In contrast, our calculations do not suggest a major input of low-$\delta^{15}N$ N north of 25°N (Figure 4a), with our region of rapid low-$\delta^{15}N$ N addition overlapping only with the more modest maximum in atmospheric N deposition near the equator. We interpret this mismatch as indicating that atmospheric N deposition is a minor contributor to the low-$\delta^{15}N$ N input to the equatorial and North Atlantic.

4.3. Agreement With Other Measures of N_2 Fixation Rate

The highest rates of N_2 fixation calculated with our approaches coincide with the rapid disappearance of "excess P" (P*) in waters upwelling in the equatorial region and flowing northward (Figures 4, 5a, and 5e). In addition, we calculate a very low N_2 fixation rate for the subtropical gyre, a region of net downwelling characterized by low P* (high N*) extending down to 700 m. Consistent with these findings, both the distribution and whole-Atlantic rate of N_2 fixation calculated by our approaches are remarkably consistent with those inferred from N-to-P relationship changes in ocean models (Table 2 and Figure 5c; Coles & Hood, 2007; Deutsch et al., 2007). Our results therefore support the hypothesis that the total rate of N_2 fixation in the Atlantic basin as a whole is set by net import and supply of excess P* to Atlantic surface waters (Deutsch et al., 2007; Straub et al., 2013).

The agreement between our reconstructions of the Atlantic basin N_2 fixation and the model simulations constrained by nutrient distributions indicates that a key assumption in the excess P-based estimates—that phytoplankton maintain a constant N/P ratio close to that of Redfield stoichiometry—does not invalidate those estimates. There is evidence for substantial variation in phytoplankton N-to-P across oceanic regions, which would tend to require higher N_2 fixation rates than under the assumption of uniform phytoplankton N-to-P (Weber & Deutsch, 2012). The agreement between our estimates and N-to-P-constrained model calculations would appear to indicate that the systematic errors in N_2 fixation rate due to the assumption of constant phytoplankton N-to-P are low. This is arguably expected, following the same logic as presented above with regard to the lack of strong effect of nitrate assimilation on our δ^{15}N-based approach for estimating N_2 fixation. On a regionally specific note, Palter et al. (2011) argue that the Gulf Stream and Ekman transport from its surface waters can supply significant excess P to the interior of the North Atlantic subtropical gyre, driving N_2 fixation. This potential effect does not appear to be important in our results or in output from physical-biogeochemical models constrained by P* (or, identically, N*) data (Coles & Hood, 2007; Deutsch et al., 2007). This disagreement calls for further investigation.

Our approach appears to agree, in terms of the spatial pattern in N_2 fixation, with a recent compilation of decades of shipboard incubation data on N_2 fixation (Figure 5b; Luo et al., 2014). One feature of our calculated N_2 fixation distribution that is not clearly supported by the compilation of incubation-based rates, however, is the high N_2 fixation rate associated with the equatorial zone (Figures 5a–5c). This may simply reflect a lack of incubation data from the eastern and central equatorial Atlantic (Sohm et al., 2011; Subramaniam et al., 2013). Analysis of the incubation results leads to an estimated N_2 fixation rate for the Atlantic of ~14 Tg N/yr (Luo et al., 2014), less than half of our estimate. The authors identify a method artifact (incomplete dissolution of the $^{15}N_2$ tracer) as a potential source of rate underestimates in their study (see Großkopf et al., 2012). In any case, the overall agreement of large-scale spatial distributions provides additional support for the view that a robust picture of N_2 fixation in the Atlantic has emerged. This intensifies the mystery of why some of these same techniques appear to disagree in the South Pacific (Gruber, 2016; Knapp et al., 2016).

4.4. Controls on N_2 Fixation

These results yield additional insight into the controls on N_2 fixation. The reconstructed distribution of N_2 fixation argues that, for the North Atlantic, N_2 fixation responds dominantly to P-bearing, N-deplete conditions. Conversely, the results argue against a dominant role for either iron limitation or temperature constraints on N_2 fixation in equatorial and northern Atlantic surface waters. The equatorial and North Atlantic receive substantial dust-borne and margin iron inputs, and both regions are typically characterized by high iron concentrations in surface waters (Figure 5f; Schlosser et al., 2014). Thus, the lack of evidence for iron limitation of N_2 fixation in these regions is perhaps not surprising. Nonetheless, our results do not preclude the possibility of iron limitation of N_2 fixation in other ocean regions with lower iron inputs.

Within the South Atlantic, hydrographic data suggest the availability of substantial excess P in the euphotic zone (Figure 5e). Our isotope-based constraint of 2–4 Tg N/yr of N_2 fixation between 30°S and 11°S concurs with previous P*-based calculations that suggest that N_2 fixation inputs are minor in the South Atlantic (e.g., Deutsch et al., 2007). This implies that excess P availability is not adequate to drive N_2 fixation in

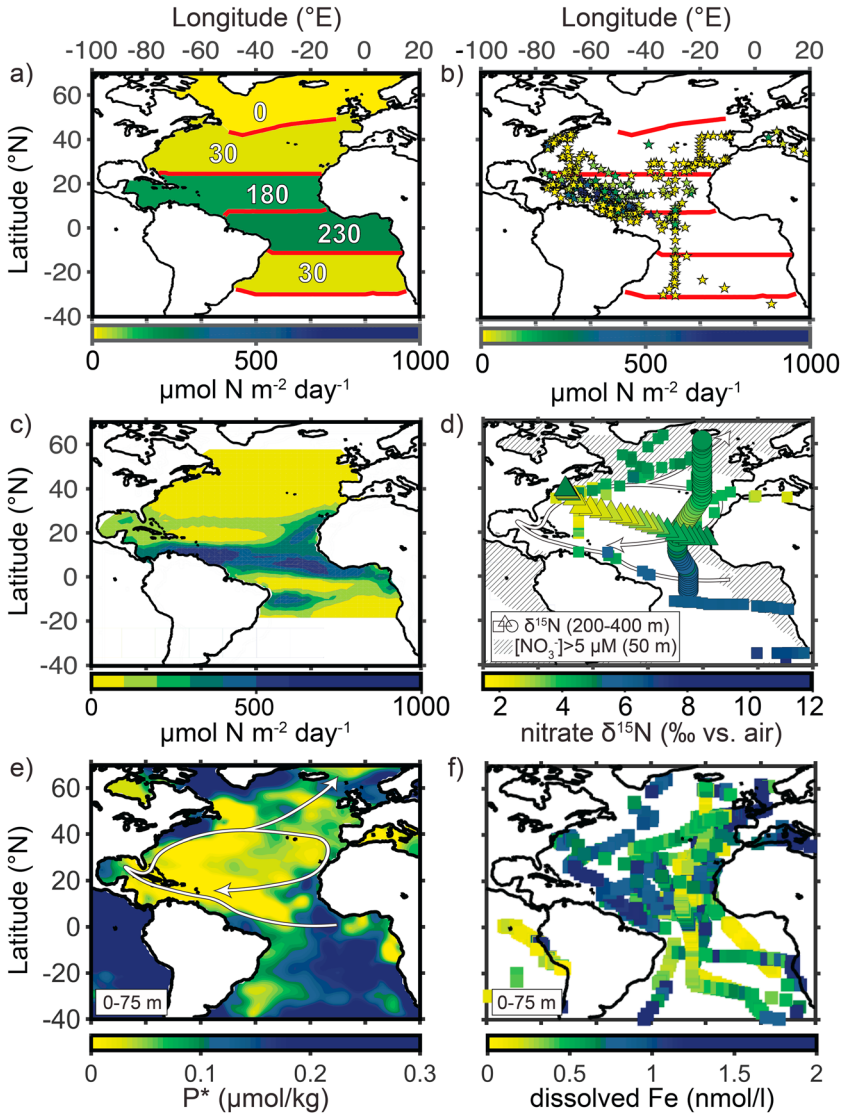

Figure 5. Comparison of our results with the Atlantic distributions of nitrate $\delta^{15}N$, with previous estimates of N_2 fixation from shipboard incubations and a model-based approach and with potential influences on N_2 fixation in the basin (excess P (P*) and dissolved iron concentrations). (a) Area-normalized N_2 fixation rates for the Atlantic converted from the area-integral rates of Figure 4, combining the results shown in Figures 4a and 4b. (b) A compilation of shipboard incubation measurements of N_2 fixation rate (Luo et al., 2014). (c) A model-based estimate of Atlantic N_2 fixation (Coles & Hood, 2007; their NSTAR run). (d) Atlantic distribution of nitrate $\delta^{15}N$ for samples below the euphotic zone (200 m to 400 m depth). Filled circles and triangles indicate nitrate $\delta^{15}N$ measurements along the A16N and GA03 transects, respectively. Filled squares in the southern hemisphere indicate nitrate $\delta^{15}N$ measurements along the CoFeMUG transect (~11°S) and along the SAMBA transect (~30°S). Filled squares in the Northern Hemisphere include nitrate $\delta^{15}N$ measurements performed for stations and along multiple transects in the North Atlantic: Transects from the western tropical North Atlantic to the subarctic North Atlantic (Van Oostende et al., 2017), the Bermuda Atlantic Time Series (BATS) and along BVAL (the BATS validation transect) in the western North Atlantic (Knapp et al., 2005, 2008), the CLIvar Mode water Dynamics Experiment (CLIMODE) across the Gulf Stream region, stations in the Brazil Current that were part of Marine Nitrogen fixation and Tropospheric Responses to Aeolian Inputs (MANTRA), the eastern subtropical North Atlantic (Bourbonnais et al., 2009), the U.S. GEOTRACES transect in the eastern subtropical North Atlantic (Casciotti et al., 2016), and the Mediterranean Sea (Pantoja et al., 2002). The hatch marks indicate regions with surface (<50 m depth) waters containing nitrate concentrations greater than 5 μmol/kg (https://odv.awi.de/en/data/ocean/woce_global_hydrographic_climatology/). White arrows indicate the main features of the shallow circulation. (e) The distribution of P* obtained by averaging P* fields at 0 m, 25 m, 50 m, and 75 m. (f) Measurements of dissolved iron displayed for shallow waters between 0 m and 75 m (colored-filled squares) (http://pcwww.liv.ac.uk/~atagliab/LIV_WEB/Data.html).

Table 2
Estimates of N_2 Fixation in the Atlantic Ocean, Sorted by Latitude

Domain	Rate (Tg N/yr)	Reference	Method
Atlantic (north of 24°N)	3	This study	Nitrate $\delta^{15}N$
Atlantic (10–50°N)	28	Gruber and Sarmiento (1997)	N/P
Atlantic (north of 0°N)	34	Coles and Hood (2007)	N/P plus models
Atlantic (north of 11°S)	27	This study	Nitrate $\delta^{15}N$
Atlantic (north of 25°S)	41	Coles and Hood (2007)	N/P plus models
Atlantic (north of 30°S)	31	This study	Nitrate $\delta^{15}N$
Atlantic (35°S–50°N)	24	Moore et al. (2009)	N/P
Atlantic (35°S–35°N)	22	Hansell et al. (2007)	N/P
Atlantic (north of 45°S)	28	Fonseca-Batista et al. (2017)	Tracer ^{15}N
Atlantic (45°S–45°N)	28	Deutsch et al. (2007)	N/P
Atlantic (45°S–45°N)	15–24	Knapp et al. (2008)	Nitrate $\delta^{15}N$

the South Atlantic and, therefore, that additional limitations from lack of iron supply (yellow regions in Figure 5f) and/or physical conditions may be important in this region. Given the net northward transport of the shallow water column through the Atlantic, this "missed opportunity" for N_2 fixation in the South Atlantic likely enhances the flux of upper ocean excess P into the North Atlantic and, by extension, the N_2 fixation that occurs there (Moore et al., 2009; Schlosser et al., 2014).

The total rate of N_2 fixation calculated for the Atlantic has implications for controls on N_2 fixation elsewhere in the global ocean, through consideration of the global ocean's fixed N budget. The ~30 Tg N/yr calculated for the Atlantic indicates that Atlantic N_2 fixation is a small fraction of the global N_2 fixation rate (estimated to be 120–140 Tg N/yr; Codispoti,2007; Deutsch et al., 2007). Moreover, this rate is not vastly greater than model-based estimates of N loss by benthic denitrification for the Atlantic basin (e.g., ~16 Tg N/yr by DeVries et al., 2013). These findings suggest that Atlantic N_2 fixation currently does not play a major role in compensating for N loss in the rest of the ocean. This implies that N loss occurring outside the Atlantic is largely compensated for by N_2 fixation in those basins. The Atlantic has the highest area-normalized rate of dust-borne iron input among the major ocean basins, and iron limitation of N_2 fixation may be important in some regions of the other basins (e.g., the eastern and central South Pacific; Knapp et al., 2016). Nevertheless, the implied coupling of N loss and N_2 fixation in the non-Atlantic basins argues that there are adequately extensive regions in those basins where iron does not limit N_2 fixation, such as the western North Pacific margins and contiguous open ocean region downstream of the Asian dust sources, to eventually remove basin-wide excess P. This result is consistent with the nutrient ratio-based assessment of Deutsch et al. (2007).

Our findings for the modern ocean are supported by paleoceanographic evidence from the tropical North Atlantic covering the last 160,000 years. The shell-bound organic nitrogen $\delta^{15}N$ of planktonic foraminifera points to changes in the circulation-driven supply of excess P to the Atlantic surface as the dominant driver of past changes in North Atlantic N_2 fixation (Straub et al., 2013). Over the same time period, there were substantial changes in water column denitrification in the Indo-Pacific (e.g., Liu et al., 2005), yet this does not appear to have influenced Atlantic N_2 fixation. This suggests that Indo-Pacific variations in N loss were compensated within those basins, minimizing their capacity to affect excess P supply to the North Atlantic.

Nevertheless, the finding that N_2 fixation in the equatorial and tropical Atlantic primarily responds to the supply of excess P has important implications for the stability of the fixed N budget in the modern and past ocean. Most of the ocean flows through the tropical Atlantic surface in less than 2,500 years (as calculated by dividing the ocean volume by the volume transport of the Brazil Current). Based on current inputs of iron to the North Atlantic, imbalances between N loss and N_2 fixation in other basins would be compensated for within the North Atlantic on this time scale. The residence time of fixed N in the global ocean appears to be roughly 3,000 years (e.g., Deutsch et al., 2004; Eugster & Gruber, 2012), such that the compensating role for North Atlantic N_2 fixation would be effective at maintaining a balance between fixed N inputs and outputs, thus stabilizing the N-to-P ratio of the global ocean. Coupled physical-biogeochemical models could investigate this hypothesis.

4.5. Offset Distributions of Lowest Nitrate $\delta^{15}N$ and Highest N_2 Fixation

The distribution of N_2 fixation reconstructed here is not identical to the distribution of nitrate $\delta^{15}N$ in the basin (Figures 4, 5a, and 5d). Specifically, the equatorial region of high N_2 fixation is offset southward from the minimum in nitrate $\delta^{15}N$ that is apparently centered in the North Atlantic subtropical gyre (Figures 4, 5a, and 5d). Similarly, Deutsch et al. (2007) and Coles and Hood (2007) showed a southward offset of the maximum in N_2 fixation rates from the North Atlantic N* maximum (Figure 5c). While this spatial offset may seem surprising at first, it has a straightforward explanation (Knapp et al., 2008): excess P is supplied largely from the south, and the N_2 fixation that responds to it progressively adds low-$\delta^{15}N$ nitrate to the shallow subsurface nitrate pool as the horizontal circulation carries surface and middepth waters northward. Moreover, the amplitude of the nitrate $\delta^{15}N$ decline is strongly influenced by circulation-associated nitrate concentration variations, such that nitrate $\delta^{15}N$ is lowest in the western subtropical North Atlantic, where the thermocline nitrate concentration is lowest (Marconi et al., 2015). In short, the low $\delta^{15}N$ nitrate observed in the subtropical gyre is a regional—not a local—signal of N_2 fixation (Knapp et al., 2005). This has important implications for studies using the N isotopes in the Atlantic. For example, the low $\delta^{15}N$ of organic N observed at high trophic levels in the North Atlantic subtropical gyre has been interpreted as the result of grazing on diazotrophs (Mompeán et al., 2016). However, the low $\delta^{15}N$ of these higher trophic levels is better explained by grazing on a broader range of phytoplankton that have assimilated the low-$\delta^{15}N$ nitrate supplied to the subtropical North Atlantic surface waters. The low $\delta^{15}N$ of this nitrate is itself a regional signal of prior N_2 fixation that occurred predominantly in the equatorial and tropical North Atlantic.

5. Conclusions

We provide new estimates of the rate and spatial distribution of Atlantic N_2 fixation based on the difference between the $\delta^{15}N$ of northward- and southward-transported nitrate calculated across five WOCE sections (from 30°S to 48°N). By combining nitrate isotope differences with the gross southward nitrate fluxes from volume transports, we avoid the proportionally large uncertainty in the net difference between the two large (northward and southward) transports. Thus, this study demonstrates a novel general strategy for using of hydrographic section transport estimates to map ocean biogeochemical fluxes.

The greatest $\delta^{15}N$ difference between northward- and southward-transported nitrate is observed between 11°S and 24°N, indicating that ~90% of the N_2 fixation rate calculated for the Atlantic basin (~30 Tg N/yr) is focused in the equatorial and tropical North Atlantic. The equatorial focusing of N_2 fixation is not coincident with regions of greatest atmospheric N deposition as derived from atmospheric models, arguing against a major role for anthropogenic atmospheric N input in driving the low $\delta^{15}N$ of nitrate observed in the Atlantic.

The relatively small N_2 fixation input to the subtropical North Atlantic and in the South Atlantic cannot be explained by a single limiting factor. In the North Atlantic, our calculations suggest that N_2 fixation dominantly responds to P-bearing, N-deplete conditions, pointing to the importance of the supply of excess P in driving N_2 fixation and arguing against iron as a major control on N_2 fixation in this region. In the South Atlantic, the N_2 fixation input is small despite of the apparent availability of substantial excess P. This implies a constraint from limited iron supply or some other (e.g., physical) condition. However, since most of the upper water column in the South Atlantic eventually flows northward, N_2 fixation in the North Atlantic should compensate for this constraint on N_2 fixation in the South Atlantic.

Our estimate of ~30 Tg N/yr for Atlantic N_2 fixation implies that the Atlantic is not a dominant contributor to global ocean N_2 fixation (estimated at 120–140 Tg N/yr; Codispoti, 2007; Deutsch et al., 2007), such that the Atlantic currently does not play a major role in compensating for N loss in the rest of the modern ocean. This suggests that the N loss occurring outside the Atlantic is largely compensated for by N_2 fixation in those basins. However, if the other basins were at some time to develop an imbalance between N input and loss, upper ocean flow through the Atlantic would modulate N_2 fixation within the basin so as to compensate for the imbalance. Since this process occurs on a shorter time scale than the residence time of fixed N in the ocean, it should effectively stabilize the N-to-P ratio of the global ocean.

Acknowledgments

We thank chief scientists Molly O. Baringer and John L. Bullister and the crew of the R/V *Ronald H. Brown* and Charles Fischer and Eric Wisegarver for sample collection from the ODF rosette during A16N. We thank chief scientist Sandy Thomalla and the crew of the R/V *S.A. Agulhas II*, as well as Isabelle Ansorge, Preston Kemeny, and Sandi Smart for help with sample collection along SAMBA. We thank chief scientist Mak Saito, as well as Caitlin Frame and Matthew McIlvin for collection and analysis of nitrate isotope samples from the CoFeMUG section. Data from the CoFeMUG section are available at http://www.bco-dmo.org. We thank Sergey Oleynik for technical assistance with the mass spectrometer at Princeton, Alexander Ganachaud and Natalie M. Mahowald for providing the transports and the dust deposition data sets, and Mathis Hain for discussions. This work was supported by the U. S. NSF through grant 0960802 to D. M. S., grant 1136345 to B. B. W. and D. M. S, grant 0526277 to K. L. C., and grant NSF-OCE 1537314 to A. N. K. Support was also provided by the Grand Challenges Program at Princeton University.

References

Alkhatib, M., Lehmann, M. F., & del Giorgio, P. A. (2012). The nitrogen isotope effect of benthic remineralization-nitrification-denitrification coupling in an estuarine environment. *Biogeosciences*, *9*, 1633–1646.

Altieri, K. E., Fawcett, S. E., Peters, A. J., Sigman, D. M., & Hastings, M. G. (2016). Marine biogenic source of atmospheric organic nitrogen in the subtropical North Atlantic. *Proceedings of the National Academy of Sciences*, *113*(4), 925–930.

Ansorge, I. J., Baringer, M. O., Campos, E. J. D., Dong, S., Fine, R. A., Garzoli, S. L., … Van den Berg, M. A. (2014). Basin-wide oceanography array bridges the South Atlantic. *Eos, Transactions American Geophysical Union*, *95*(6), 53–54.

Bianchi, D., Dunne, J. D., Sarmiento, J. L., & Galbraith, E. D. (2012). Data-based estimates of suboxia, denitrification, and N_2O production in the ocean and their sensitivities to dissolved O_2. *Global Biogeochemical Cycles*, *26*, GB2009. https://doi.org/10.1029/2011GB004209

Biastoch, A., Boning, C. W., & Lutjeharms, J. R. E. (2008). Agulhas leakage dynamics affects decadal variability in Atlantic overturning circulation. *Nature*, *456*, 489–492.

Bourbonnais, A., Lehmann, M. F., Waniek, J. J., & Schulz-Bull, D. E. (2009). Nitrate isotope anomalies reflect N_2 fixation in the Azores Front region (subtropical NE Atlantic). *Journal of Geophysical Research*, *114*, C03003. https://doi.org/10.1029/2007JC004617

Brandes, J. A., & Devol, A. H. (1997). Isotopic fractionation of oxygen and nitrogen in coastal marine sediments. *Geochimica et Cosmochimica Acta*, *61*(9), 1793–1801.

Brandes, J. A., & Devol, A. H. (2002). A global marine fixed nitrogen isotopic budget: Implications for Holocene nitrogen cycling. *Global Biogeochemical Cycles*, *16*(4), 1120–1134.

Campbell, E. C. (2016). Where three oceans meet: Nitrate isotope measurements from the South Atlantic along 34.5°S. Undergraduate senior thesis, Princeton University, 1–59.

Capone, D. G., Subramaniam, A., Montoya, J. P., Voss, M., Humborg, C., Johansen, A. M., … Carpenter, E. J. (1998). An extensive bloom of the N-2-fixing cyanobacterium Trichodesmium erythraeum in the central Arabian Sea. *Marine Ecology Progress Series*, *172*, 281–292.

Carpenter, E. J., Harvey, H. R., & Fry, B. (1997). Biogeochemical tracers of the marine cyanobacterium Trichodesmium. *Deep Sea Research, Part I*, *44*, 27–38.

Carpenter, E. J., & McCarthy, J. J. (1975). Nitrogen fixation and uptake of combined nitrogenous nutrients by *Oscillatoria (Trichodesmium) thiebautii* in the western Sargasso Sea. *Limnology and Oceanography*, *20*, 389–401.

Carpenter, E. J., & Price, C. C. (1976). Marine *Oscillatoria* (*Trichodesmium*): Explanation for aerobic nitrogen fixation without heterocysts. *Science*, *191*, 1278–1280.

Carpenter, E. J., & Price, C. C. (1977). Nitrogen fixation, distribution and production of *Oscillatoria (Trichodesmium)* spp. in the Western Sargasso and Caribbean Sea. *Limnology and Oceanography*, *22*, 60–72.

Carpenter, E. J., & Romans, K. (1991). Major role of the cyanobacterium *Trichodesmium* in nutrient cycling in the North Atlantic Ocean. *Science*, *254*, 1356–1358.

Casciotti, K., McIlvin, M. R., Forbes, M. S., & Sigman, D. (2016). *Nitrate Isotopes of Nitrate in the GEOTRACES North Atantic Zonal Transect—Casciotti Laboratory*. UK: British Oceanographic Data Centre - Natural Environment Research Council.

Casciotti, K. L., Sigman, D. M., Hastings, M. G., Bohlke, J. K., & Hilkert, A. (2002). Measurement of the oxygen isotopic composition of nitrate in seawater and freshwater using the denitrifier method. *Analytical Chemistry*, *74*(19), 4905–4912.

Casciotti, K. L., Trull, T. W., Glover, D. M., & Davies, D. (2008). Constraints on nitrogen cycling at the sub-tropical North Pacific Station ALOHA from isotopic measurements of nitrate and particulate nitrogen. *Deep Sea Research, Part II*, *55*, 1661–1672.

Chien, C. T., Mackey, K. R. M., Dutkiewicz, S., Mahowald, N. M., Prospero, J. M., & Paytan, A. (2016). Effects of African dust deposition on phytoplankton in the western tropical Atlantic Ocean off Barbados. *Global Biogeochemical Cycles*, *30*, 716–734.

Cline, J. D., & Kaplan, I. R. (1975). Isotopic fractionation of dissolved nitrate during denitrification in the Eastern Tropical North Pacific Ocean. *Marine Chemistry*, *3*, 271–299.

Codispoti, L. (2007). An oceanic fixed nitrogen sink exceeding 400 Tg N a^{-1} vs. the concept of homeostasis in the fixed-nitrogen inventory. *Biogeosciences*, *4*, 233–253.

Codispoti, L. A., Brandes, J. A., Christensen, J. P., Devol, A. H., Naqvi, S. W. A., Paerl, H. W., & Yoshinari, T. (2001). The oceanic fixed nitrogen and nitrous oxide budgets: Moving targets as we enter the Anthropocene? *Scientia Marina*, *65*, 85–105.

Coles, V. J., & Hood, R. R. (2007). Modeling the impact of iron and phosphorus limitations on nitrogen fixation in the Atlantic Ocean. *Biogeosciences*, *4*, 455–479.

Delwiche, C. C., Zinke, P. J., Johnson, C. M., & Virginia, R. A. (1979). Nitrogen isotope distribution as a presumptive indicator of nitrogen-fixation. *Botanical Gazette*, *140*, 65–69.

Dencausse, G., Arhan, M., & Speich, S. (2010). Routes of Agulhas rings in the southeastern Cape Basin. *Deep Sea Research, Part II*, *57*, 1406–1421.

Dentener, F., Drevet, J., Lamarque, J. F., Bey, I., Eickhout, B., Fiore, A. M., … Wild, O. (2006). Nitrogen and sulfur deposition on regional and global scales: A multimodel evaluation. *Global Biogeochemical Cycles*, *20*, GB4003. https://doi.org/10.1029/2005GB002672

Deutsch, C., Sarmiento, J. L., Sigman, D. M., Gruber, N., & Dunne, J. P. (2007). Spatial coupling of nitrogen inputs and losses in the ocean. *Nature*, *445*, 163–167.

Deutsch, C., Sigman, D. M., Thunell, R. C., Meckler, A. N., & Haug, G. H. (2004). Isotopic constraints on glacial/interglacial changes in the oceanic nitrogen budget. *Global Biogeochemical Cycles*, *18*, GB4012. https://doi.org/10.1029/2003GB002189

DeVries, T., Deutsch, C., Rafter, P. A., & Primeau, F. (2013). Marine denitrification rates determined from a global 3-dimensional inverse model. *Biogeosciences*, *10*, 2481–2496.

Dugdale, R. C., Goering, J. J., & Ryther, J. H. (1964). High nitrogen fixation rates in the Sargasso Sea and the Arabian Sea. *Limnology and Oceanography*, *9*, 507–510.

Eugster, O., & Gruber, N. (2012). A probabilistic estimate of global marine N-fixation and denitrification. *Global Biogeochemical Cycles*, *26*, GB4013. https://doi.org/10.1029/2012GB004300

Falkowski, P. G. (1997). Evolution of the nitrogen cycle and its influence on the biological sequestration of CO_2 in the ocean. *Nature*, *387*, 272–275.

Fonseca-Batista, D., Dehairs, F., Riou, V., Fripiat, F., Elskens, M., Deman, F., … Auel, H. (2017). Nitrogen fixation in the eastern Atlantic reaches similar levels in the Southern and Northern Hemisphere. *Journal of Geophysical Research: Oceans*, *122*, 587–601. https://doi.org/10.1002/2016JC012335

Ganachaud, A. (2003). Large-scale mass transports, water mass formation, and diffusivities estimated from World Ocean Circulation Experiment (WOCE) hydrographic data. *Journal of Geophysical Research*, *108*, 3213. https://doi.org/10.1029/2002JC001565

Ganachaud, A., & Wunsch, C. (2000). Improved estimates of global ocean circulation, heat transport and mixing from hydrographic data. *Nature*, *408*, 453–456.

Ganachaud, A., & Wunsch, C. (2002). Oceanic nutrient and oxygen fluxes during the World Ocean Circulation Experiment and bounds on export production. *Global Biogeochemical Cycles*, *16*(4), 1057. https://doi.org/10.1029/2000GB001333

Gordon, A. (1986). Interocean exchange of thermocline water. *Journal of Geophysical Research*, *91*(4), 5037–5046. https://doi.org/10.1029/JC091iC04p05037

Granger, J., Prokopenko, M. G., Sigman, D. M., Mordy, C. W., Morse, Z. M., Morales, L. W., … Plessen, B. (2011). Coupled nitrification-denitrification in sediment of the eastern Bering Sea shelf leads to ^{15}N enrichment of fixed N in shelf waters. *Journal of Geophysical Research*, *116*, C11006. https://doi.org/10.1029/2010JC006751

Großkopf, T., Mohr, W., Baustian, T., Schunck, H., Gill, D., Kuypers, M. M. M., … LaRoche, J. (2012). Doubling of marine dinitrogen-fixation rates based on direct measurements. *Nature*, *488*, 361–364.

Gruber, N. (2004). The dynamics of the marine nitrogen cycle and its influence on atmospheric CO_2 variations. In M. F. A. T. Oguz (Ed.), *Carbon-Climate Interactions* (pp. 1–39). New York: Wiley.

Gruber, N. (2016). Elusive marine nitrogen fixation. *Proceedings of the National Academy of Sciences*, *113*(16), 4246–4248.

Gruber, N., & Sarmiento, J. L. (1997). Global patterns of marine nitrogen fixation and denitrification. *Global Biogeochemical Cycles*, *11*(2), 235–266.

Hansell, D. A., & Follows, M. J. (2008). Nitrogen in the Atlantic Ocean. In M. Mulholland, D. Bronk, D. Capone, & E. Carpenter (Eds.), *Nitrogen in the Marine Environment* (pp. 597–630). Burlington, MA: Academic Press.

Hansell, D. A., Bates, N. R., & Olson, D. B. (2004). Excess nitrate and nitrogen fixation in the North Atlantic Ocean. *Marine Chemistry*, *84*, 243–265.

Hansell, D. A., Olson, D. B., Dentener, F., & Zamora, L. M. (2007). Assessment of excess nitrate development in the subtropical North Atlantic. *Marine Chemistry*, *106*(3–4), 562–579.

Hastings, M. G., & Sigman, D. M. (2003). Isotopic evidence for source changes of nitrate in rain at Bermuda. *Journal of Geophysical Research*, *108*(D24), 4790. https://doi.org/10.1029/2003JD003789

Hoering, T., & Ford, H. T. (1960). The isotope effect in the fixation of nitrogen by Azotobacter. *Journal of the American Chemical Society*, *82*, 376–378.

Karl, D., Michaels, A., Bergman, B., Capone, D., Carpenter, E., Letelier, F., … Stal, L. (2002). Dinitrogen fixation in the world's oceans. *Biogeochemistry*, *57*, 47–98.

Karstensen, J., Stramma, L., & Visbeck, M. (2008). Oxygen minimum zones in the eastern tropical Atlantic and Pacific oceans. *Progress in Oceanography*, *77*, 331–350.

Knapp, A. N., Casciotti, K. L., Berelson, W. M., Prokopenko, M. G., & Capone, D. G. (2016). Low rates of nitrogen fixation in the eastern tropical South Pacific surface waters. *Proceedings of the National Academy of Sciences*, *113*(6), 4398–4403.

Knapp, A. N., Dekaezemacker, J., Bonner, S., Sohm, J. A., & Capone, D. G. (2012). Sensitivity of *Trichodesmium erythraeum* and *Crocosphaera watsonii* abundance and N_2 fixation rates to varying NO_3^- and PO_4^{3-} concentrations in batch cultures. *Aquatic Microbiological Ecology*, *66*(3), 223–236.

Knapp, A. N., DiFiore, P. J., Deutsch, C., Sigman, D. M., & Lipschultz, F. (2008). Nitrate isotopic composition between Bermuda and Puerto Rico: Implications for N_2 fixation in the Atlantic Ocean. *Global Biogeochemical Cycles*, *22*, GB3014. https://doi.org/10.1029/2007GB003107

Knapp, A. N., Hastings, M. G., Sigman, D. M., Lipschultz, F., & Galloway, J. N. (2010). The flux and isotopic composition of reduced and total nitrogen in Bermuda rain. *Marine Chemistry*, *120*(1–4), 83–89.

Knapp, A. N., Sigman, D. M., & Lipschultz, F. (2005). N isotopic composition of dissolved organic nitrogen and nitrate at the Bermuda Atlantic time-series study site. *Global Biogeochemical Cycles*, *19*, GB1018. https://doi.org/10.1029/2004GB002320

Knapp, A. N., Sigman, D. M., Lipschultz, F., Kustka, A. B., & Capone, D. G. (2011). Interbasin isotopic correspondence between upper-ocean bulk DON and subsurface nitrate and its implications for marine nitrogen cycling. *Global Biogeochemical Cycles*, *25*, GB4004. https://doi.org/10.1029/2010GB003878

Lehmann, M. F., Sigman, D. M., & Berelson, W. M. (2004). Coupling the N-15/N-14 and O-18/O-16 of nitrate as a constraint on benthic nitrogen cycling. *Marine Chemistry*, *88*(1–2), 1–20.

Lehmann, M. F., Sigman, D. M., McCorkle, D. C., Brunelle, B. G., Hoffmann, S., Kienast, M., … Clement, J. (2005). The origin of the deep Bering Sea nitrate deficit—Constraints from the nitrogen and oxygen isotopic composition of water column nitrate and benthic nitrate fluxes. *Global Biogeochemical Cycles*, *19*, GB4005. https://doi.org/10.1029/2005GB002508

Lehmann, M. F., Sigman, D. M., McCorkle, D. C., Granger, J., Hoffmann, S., Cane, G., & Brunelle, B. G. (2007). The distribution of nitrate $^{15}N/^{14}N$ in marine sediments and the impact of benthic nitrogen loss on the isotopic composition of oceanic nitrate. *Geochimica et Cosmochimica Acta*, *71*, 5384–5404.

Liu, Z., Altabet, M. A., & Herbert, T. D. (2005). Glacial-interglacial modulation of eastern tropical North Pacific denitrification over the last 1.8-Myr. *Geophysical Research Letters*, *32*, L23607. https://doi.org/10.1029/2005GL024439

Liu, K. K., Su, M. J., Hsueh, C. R., & Gong, G. C. (1996). The nitrogen isotopic composition of nitrate in the Kuroshio Water northwest of Taiwan: Evidence for nitrogen fixation as a source of isotopically light nitrate. *Marine Chemistry*, *54*, 273–292.

Luo, Y. -W., Lima, I. D., Karl, D. M., Deutsch, C. A., & Doney, S. C. (2014). Data-based assessment of environmental controls on global marine nitrogen fixation. *Biogeosciences*, *11*, 691–708.

Marconi, D. (2017). Use of the nitrate isotopes in the ocean interior to explore the isotopic composition of sinking nitrogen and its implications for marine biogeochemical cycles. Doctoral dissertation, Princeton University, 1–319.

Marconi, D., Weigand, M. A., Rafter, P. A., McIlvin, M. R., Forbes, M., Casciotti, K. L., & Sigman, D. M. (2015). Nitrate isotope distributions on the US GEOTRACES North Atlantic cross-basin section: Signals of polar nitrate sources and low latitude nitrogen cycling. *Marine Chemistry*, *177*(1), 143–156.

Martiny, A. C., Pham, C. T. A., Primeau, F. W., Vrugt, J. A., Moore, J. K., Levin, S. A., & Lomas, M. W. (2013). Strong latitudinal patterns in the elemental ratios of marine plankton and organic matter. *Nature Geoscience*, *6*, 279–283.

McIlvin, R. M., & Casciotti, K. L. (2011). Technical updates to the bacterial method for nitrate isotopic analyses. *Analytical Chemistry*, *83*(5), 1850–1856.

Michaels, A. F., Olson, D., Sarmiento, J. L., Ammerman, J. W., Fanning, K., Jahnke, R., … Prospero, J. M. (1996). Inputs, losses and transformations of nitrogen and phosphorus in the pelagic north Atlantic ocean. *Biogeochemistry*, *35*, 181–226.

Mills, M. M., & Arrigo, K. R. (2010). Non-Redfield N:P utilization by phytoplankton significantly impacts oceanic nitrogen fixation. *Nature Geoscience*, *3*, 412–416.

Minagawa, M., & Wada, E. (1986). Nitrogen isotope ratios of red tide organisms in the East China Sea: A characterization of biological nitrogen fixation. *Marine Chemistry*, *19*, 245–259.

Mompeán, C., Bode, A., Gier, E., & McCarthy, M. D. (2016). Bulk vs. amino acid stable N isotope estimations of metabolic status and contributions of nitrogen fixation to size-fractionated zooplankton biomass in the subtropical N Atlantic. *Deep Sea Research Part I*, *114*, 137–148.

Monteiro, F. M., Dutkiewicz, S., & Follows, M. J. (2011). Biogeographical controls on the marine nitrogen fixers. *Global Biogeochemical Cycles*, *25*, GB2003. https://doi.org/10.1029/2010GB003902

Montoya, J. P., Carpenter, E. J., & Capone, D. G. (2002). Nitrogen-fixation and nitrogen isotope abundances in zooplankton of the oligotrophic North Atlantic. *Limnology and Oceanography*, *47*, 1617–1628.

Moore, C. M., Mills, M. M., Achterberg, E. P., Geider, R. J., LaRoche, J., Lucas, M. I., … Woodward, E. M. S. (2009). Large-scale distribution of Atlantic nitrogen fixation controlled by iron availability. *Nature Geoscience*, *2*, 867–871.

Olsen, A., Key, R. M., van Heuven, S., Lauvset, S. K., Velo, A., Lin, X., … Suzuki, T. (2016). The Global Ocean Data Analysis Project version 2 (GLODAPv2)—An internally consistent data product for the world ocean. *Earth System Science Data*, *8*, 297–323.

Palter, J. B., Lozier, M. S., Sarmiento, J. L., & Williams, R. G. (2011). The supply of excess phosphate across the Gulf Stream and the maintenance of subtropical nitrogen fixation. *Global Biogeochemical Cycles*, *25*, GB4007. https://doi.org/10.1029/2010GB003955

Pantoja, S., Repeta, D. J., Sachs, J. P., & Sigman, D. M. (2002). Stable isotope constraints on the nitrogen cycle of the Mediterranean Sea water column. *Deep Sea Research Part I: Oceanographic Research Papers*, *49*(9), 1609–1621.

Rafter, P. A., & Sigman, D. M. (2016). Spatial distribution and temporal variation of nitrate nitrogen and oxygen isotopes in the upper equatorial Pacific Ocean. *Limnology and Oceanography*, *61*(1), 14–31.

Sanudo-Wilhemly, S. A., Tovar-Sanchez, A., Fu, F. X., Capone, D. G., Carpenter, E. J., & Hutchins, D. A. (2004). The impact of surface-adsorbed phosphorous on phytoplankton Redfield stoichiometry. *Nature*, *432*, 897–901.

Schlosser, C., Baker, A. R., Blain, S., Achterberg, E. P., Boye, M., Bowie, A. R., … Moore, C. M. (2014). Seasonal ITCZ migration dynamically controls the location of the (sub)tropical Atlantic biogeochemical divide. *PNAS*, *111*(4), 1438–1442.

Sebilo, M., Billen, G., Grably, M., & Mariotti, A. (2003). Isotopic composition of nitrate-nitrogen as a marker of riparian and benthic denitrification at the scale of the whole Seine River system. *Biogeochemistry*, *63*(1), 35–51.

Sigman, D. M., Casciotti, K. L., Andreani, M., Barford, C., Galanter, M., & Bohlke, J. K. (2001). A bacterial method for the nitrogen isotopic analysis of nitrate in seawater and freshwater. *Analytical Chemistry*, *73*(17), 4145–4153.

Sigman, D. M., DiFiore, P. J., Hain, M. P., Deutsch, C., & Karl, D. M. (2009). Sinking organic matter spreads the nitrogen isotope signal of pelagic denitrification in the North Pacific. *Geophysical Research Letters*, *36*, L08605. https://doi.org/10.1029/2008GL035784

Sigman, D. M., Granger, J., DiFiore, P., Lehmann, M. F., Geen, A. v., Ho, R., & Cane, G. (2005). Coupled nitrogen and oxygen isotope measurements of nitrate along the eastern North Pacific margin. *Global Biogeochemical Cycles*, *19*, GB4022. https://doi.org/10.1029/2005GB002458

Sohm, J. A., Hilton, J. A., Noble, A. E., Zehr, J. P., Saito, M. A., & Webb, E. A. (2011). Nitrogen fixation in the South Atlantic Gyre and the Benguela Upwelling System. *Geophysical Research Letters*, *38*, L16608. https://doi.org/10.1029/2011GL048315

Straub, M., Sigman, D. M., Ren, H., Martinez-Garcia, A., Meckler, A. N., Hain, M. P., & Haug, G. H. (2013). Changes in North Atlantic nitrogen fixation controlled by ocean circulation. *Nature*, *501*, 200–203.

Subramaniam, A., Mahaffey, C., Johns, W., & Mahowald, N. (2013). Equatorial upwelling enhances nitrogen fixation in the Atlantic Ocean. *Geophysical Research Letters*, *40*, 1766–1771. https://doi.org/10.1002/grl.50250

Turekian, V. C. (2000). The application of chemical and isotopic tracers to characterize aerosol sources and processing in marine air. Doctoral dissertation, University of Virginia, 1–192.

Van Oostende, N., Fawcett, S. E., Marconi, D., Lueders-Dumont, J., Sabadel, A. J. M., Woodward, E. M. S., … Ward, B. B. (2017). Variation of summer phytoplankton community composition and its relationship to nitrate and regenerated nitrogen assimilation across the North Atlantic Ocean. *Deep-Sea Research Part I: Oceanographic Research Papers*, *121*, 79–94.

Weber, T. S., & Deutsch, C. (2010). Ocean nutrient ratios governed by plankton biogeography. *Nature*, *467*(7315), 550–554.

Weber, T. S., & Deutsch, C. (2012). Oceanic nitrogen reservoir regulated by plankton diversity and ocean circulation. *Nature*, *489*, 419–422.

Weigand, M. A., Foriel, J., Barnett, B., Oleynik, S., & Sigman, D. M. (2016). Updates to instrumentation and protocols for isotopic analysis of nitrate by the denitrifier method. *Rapid Communications in Mass Spectrometry*, *30*, 1365–1383.

Wong, G. T. F., Chung, S. W., Shiah, F. K., Chen, C. C., Wen, L. S., & Liu, K. K. (2002). Nitrate anomally in the upper nutrientcline in the northern South China Sea—Evidence for nitrogen fixation. *Geophysical Research Letters*, *29*, 1–4. https://doi.org/10.1029/2002GL015796